ORIGINAL ARTICLE

Formulation and characterization of folate receptor-targeted PEGylated liposome encapsulating bioactive compounds from *Kappaphycus alvarezii* for cancer therapy

Suraj Baskararaj[1] · Theivendren Panneerselvam[2] · Saravanan Govindaraj[3] · Sankarganesh Arunachalam[1] · Pavadai Parasuraman[4] · Sureshbabu Ram Kumar Pandian[1] · Murugesan Sankaranarayanan[5] · Uma Priya Mohan[1] · Ponnusamy Palanisamy[6] · Vigneshwaran Ravishankar[1] · Selvaraj Kunjiappan[1]

Abstract

This study aimed to formulate and characterize the folate receptor-targeted PEGylated liposome encapsulating bioactive compounds from *Kappaphycus alvarezii* to enhance the anticancer activity. Twenty valued bioactive compounds (3-hydroxy benzoicacid, gallicacid, chlorogenicacid, cinnamicacid, artemiseole, hydrazine carbothioamide, etc.,) are confirmed from methanol extract of *K. alvarezii* using analytical techniques like HPLC and GC–MS. The delivery of bioactive compounds of *K. alvarezii* via naturally overexpressed folate receptor (FR) to FR-positive breast cancer cells was studied. FR targeted PEGylated liposome was constructed by modified thin-film hydration technique using FA-PEG-DSPE/cholesterol/DSPC (5:40:55) and bioactive compounds of *K. alvarezii* was encapsulated. Their morphology, size, shape, physiological stability and drug release kinetics were studied. The study reports of *K. alvarezii* extract-encapsulated PEGylated liposome showed spherical shaped particles with amorphous in nature. The mean diameter of *K. alvarezii* extract–encapsulated PEGylated and FA-conjugated PEGylated liposomes was found to be 110 ± 6 nm and 140 ± 5 nm, respectively. Based on the stability studies, it could be confirmed that FA-conjugated PEGylated liposome was highly stable in various physiological buffer medium. FA-conjugated PEGylated liposome can steadily release the bioactive compounds of *K. alvarezii* extract in acidic medium (pH 5.4). MTT assay demonstrated the concentration-dependent cytotoxicity against MCF-7 cells after 24 h with IC$_{50}$ of 81 µg/mL. Also, PEGylated liposome enhanced the delivery of *K. alvarezii* extract in MCF-7 cells. After treatment, typical apoptotic morphology of condensed nuclei and distorted membrane bodies was picturized. Additionally, PEGylated liposome targets the mitochondria of MCF-7 cells and significantly increased the level of ROS and contributes to the damage of mitochondrial transmembrane potential. Hence, PEGylated liposome could positively deliver the bioactive compounds of *K. alvarezii* extract into FR-positive breast cancer cells (MCF-7) and exhibit great potential in anticancer therapy.

Keywords Apoptosis · Breast cancer · Folate receptor · *Kappaphycus alvarezii* · Liposome

✉ Theivendren Panneerselvam
  tpsphc@gmail.com

✉ Murugesan Sankaranarayanan
  murugesan@pilani.bits-pilani.ac.in

✉ Selvaraj Kunjiappan
  selvapharmabio@gmail.com

Extended author information available on the last page of the article

Introduction

Nanocapsules are carriers surrounded by polymer membrane where molecules can be loaded in its inner core or its surface (Singh and Lillard Jr 2009). Various alchemy drugs (Yoo and Park 2004), enzymes (Pun et al. 2004), phytochemicals (Xie et al. 2016) and nucleic acids (Li and Szoka 2007) are delivered site specifically with nanomaterials for the in vitro and in vivo treatment of cancer. The delivery of these materials with nanoparticles helps to improve pharmacokinetic properties such as controlled release of drugs, biocompatibility, bioavailability; besides, it also helps to reduce systemic toxicity and immunogenicity of the delivered material

(Malam et al. 2009; Chowdhury et al. 2017). Liposomes, a closed spherical sac of synthetic or natural phospholipid bilayer contains a hollow sphere in its core; any hydrophilic or hydrophobic molecules can be entrapped and carried with its inner core (Kunjiappan et al. 2018a). Liposomes are generally round and 400–2.5 µm in size which displays unique physico-chemical properties that have been widely explored for various site-specific delivery applications. Physical and chemical characteristics, including permeability, charge density and steric hindrance are based on the net constituent of phospholipids (Malam et al. 2009). Subsequently, the formation of liposomes was purely based on the self-association of the amphiphilic phospholipid molecules. Additionally, surface-modified PEGylated liposomes have significant potential therapeutic applications as injectable colloidal systems for controlled drug release with long circulation in the blood (Blume and Cevc 1990; Klibanov et al. 1990; Cho et al. 2015). In this regard, the drug loading mechanism can be achieved by the following approaches (1) the choice of aqueous solution-based liposome formation with appropriate soluble drugs, (2) using solvent exchange mechanism with suitable organic solvents, (3) with lipophilic drugs, and (4) pH gradient techniques (Qiu et al. 2008). These formulations make the liposomal surface layer more comfortable for manipulating and adding appropriate molecules to its outer layer.

Multidrug resistance (MDR) is a condition appeared in cancer cells due to hefty and repeated usage of chemotherapeutics (Persidis 1999). Tumors have developed strategies to resist chemotherapy and to avoid apoptotic pathways by two main mechanisms: (1) excess use of drug efflux pumps on the cell membrane (2) increased induction of anti-apoptotic pathways by chemotherapeutic drugs. Hence, delivery of therapeutic molecule through nanoparticles can easily bypass the drug efflux pumps and can enhance the intracellular delivery of required therapeutics. Site–specific delivery of bioactive agents will be a promising strategy for cancer where conditions like MDR may reduce the efficacy of treatment. Site-specific delivery of molecules can be increased by targeting selective cellular markers to enhance efficacy, reduce toxicity and MDR of desired therapeutic agents (Zhao et al. 2008). Among other cell surface receptors, folate receptor (FR)-α is a sought-after and most promising cell surface marker accounted in various epithelial based cancer cells. Expression of folate receptors was accounted significantly on the surface of breast, lung, kidney, ovary, colon, brain cancer and myelogenous leukaemia (Low and Antony 2004). The importance of folate receptor (FR)-β has been recognized for its range of disease targets not limited to myelogenous leukaemia and chronic inflammatory diseases such as rheumatoid arthritis (Zhao et al. 2008).

Kappaphycus alvarezii is placed under the species of red algae which has been proved to be rich in its nutrients and in therapeutic level; the extracts have been used as therapeutics for various diseases like cholesterol reducer, a source of antioxidant, anti-cancer and antiviral (Sato et al. 2011; Ferraces-Casais et al. 2012; Chang et al. 2017). Extracts of *K. alvarezii* was studied against mammary cancer model and its efficacy was proved in vitro and in vivo; however, the null toxic effect was found against somatic cells of Sprague–Dawley rats (Chang et al. 2017). Shreds of evidence from various reports proved that the extracts of *K. alvarezii* inhibited the proliferation of breast, colon, liver and osteosarcoma cells (Suganya et al. 2016; Gutiérrez-Rodríguez et al. 2018). In this present study, bioactive compounds were extracted from *K. alvarezii* and were characterized by FTIR, GC–MS and HPLC methods. Furthermore, the extract was encapsulated with folate conjugated PEGylated liposome to target the overexpressed folate receptors. Additionally, the cytotoxic/apoptotic activity of PEGylated liposomes against breast cancer (MCF-7 cells) was extensively studied in vitro with MTT, DAPI, live/dead assay, mitochondrial transmembrane potential and ROS generation methods.

Experimental section

Materials and cell lines

The chemicals, cholesterol, polyethylene glycol bis amine (NH$_2$-PEG3400), acridine orange (AO), *N*-hydroxysuccinimde, *N,N*-dicyclohexylcarbodiimide, pyridine, ethidium bromide (EB), 4′,6-diamidino-2-phenylindole (DAPI), dichlorodihydro-fluorescein diacetate (DCFH-DA), rhodamine 123, fetal bovine serum (FBS), 3-(4,5-dimethyl-2-thiazolyl)-2,5-diphenyl-tetrazolium bromide (MTT), dulbecco's modified eagle's medium (DMEM), streptomycin, penicillin and dimethyl sulfoxide (DMSO) were procured in cell-culture tested grade from Himedia Laboratories Pvt. Ltd., Mumbai, India and Sigma-Aldrich, Bangalore, India. The pharmaceutical grade folic acid (97.95%) was received as a gift from Alkem Laboratories, Mumbai, India. 1,2-distearoyl phosphatidylethanolamine (DSPE) and Distearoyl phosphatidylcholine (DSPC) were obtained from Lipoid (Germany) and Avanti Polar Lipids (Alabaster, AL, USA). The remaining chemicals and reagents used for this present study were of analytical grade supplied by Thermo-Fisher, Mumbai, India. Human adenoma breast cancer cell lines (MCF-7 cells) was procured from NCCS, Pune, Maharashtra, India and maintained in DMEM medium containing 10% heat-inactivated fetal bovine serum (FBS), 1% penicillin/streptomycin and amphotericin B.

Kappaphycus alvarezii collection, extraction and characterization

Kappaphycus alvarezii, a macro red algae (Family: Solieriaceae; Division: Rhodophyta, Class: Floridophyceae) was collected from Bay of Bengal Ocean of Mandapam coastal area (longitude: 79.12° E and latitude: 9.28º N), Ramanathapuram Dist. Tamilnadu, India, during January 2018. The collected algae were thoroughly cleaned with distilled water to get rid of salt and sand particles and allowed to dry for 15 days. The dried algae were powdered, screened through 60 mesh size screen and safely stored in an airtight container for further investigations. The powdered *K. alvarezii* (50 g) was permitted to microwave-assisted extraction (microwave apparatus (CATA R) supplied by Catalyst Systems (Pune, India) attached with a magnetron of 2450 MHZ, nominal power of 850 W with 10 power levels, time controller, exhaust system, beam reflector and a stirring device) using previously optimized variables of methanol (80%), microwave power (20%), temperature (45 °C) and time (14.5 min) (Baskararaj et al. 2019). The resultant extract was filtered and freeze-dried for further characterization. Then, FT-IR, Gas Chromatography-Mass Spectrum (GC–MS) and High-Performance Liquid Chromatography (HPLC) are used for the identification of biologically important compounds present in the extract.

Synthesis of folic acid-PEG-DSPE conjugate (FA-PEG-DSPE)

The synthesis of FA-PEG-DSPE conjugate was performed in three steps as described earlier (Gabizon et al. 1999) and following is the route map presented in Fig. 1 (scheme).

Synthesis of FA-PEG-NH$_2$

All the reaction conditions needed for the synthesis of conjugate molecules are performed in dark to avoid degradation of folicacid. First, FA-PEG-NH$_2$ was synthesized by reacting 500 mg (0.15 mmol) polyethylene glycol bis amine (NH$_2$-PEG3400) with an equimolar quantity of FA (500 mg; 1.18 mmol) in 5 mL of DMSO containing one mmol equivalent of *N, N*-dicyclohexylcarbodiimide (184 mg; 1 mmol) and 10 μL pyridine. The mixture was activated in a thermostat water bath at 40 °C and stirred overnight at 80 rpm. Then, 10 mL of water was added and the insoluble by-product (dicyclohexylurea) was removed by centrifugation. DMSO and un-reacted FA from supernatant of FA-PEG-NH$_2$ were removed by dialyzed against 5 mM NaHCO$_3$ buffer (pH 9.0) and then against deionized water. The product FA-PEG-NH$_2$ was then lyophilized and analyzed for folate and -NH$_2$ contents by thin-layer chromatographic method (TLC).

Synthesis of *N*-succinyl-DSPE

Second, *N*-succinyl-DSPE was synthesized by reacting 1.1 molar concentration of NHS (0.12 g) and 100 mg of DSPE in 5 mL chloroform containing 10 μL pyridine at room temperature under stirring condition. The product was precipitated with ice-cold acetone and confirmed by thin-layer chromatography (TLC).

Synthesis of FA-PEG-DSPE

Third, FA-PEG-DSPE conjugate was synthesized by *N*-succinyl-DSPE re-dissolved in chloroform and its carboxyl group was activated by reacting with one molar equivalent of *N, N*-dicyclohexylcarbodiimide for 4 h at room temperature. An equimolar amount of the above-synthesized FA-PEG-NH$_2$ dissolved in chloroform was then added. After overnight stirring at room temperature, the solvent was removed from the reaction mixture and the lipid pellet containing FA-PEG-DSPE conjugate was washed twice with ice-cold acetone, re-dissolved in chloroform and stored at − -20 °C. The formation of FA-PEG-DSPE was confirmed by FT-IR and proton NMR.

Formulation of *K. alvarezii* extract-encapsulated control and PEGylated liposome

Control and FA-conjugated PEGylated liposomes encapsulated *K. alvarezii* extract was formulated with slightly modified thin-film hydration technique (Zhu et al. 2013). In detail, 100 mg of mixture of lipids, FA-PEG-DSPE/cholesterol/DSPC (5:40:55) was dissolved in 10 mL mixture of methanol: chloroform (2:1), followed by removal of solvents using rotary vacuum evaporator (Buchi Rotavap). The dried lipid mixture was then re-hydrated in 2 mL of low-pH 'trapping' buffer (400 mM citrate, 5 mM phosphate, pH 4.0) by vortexing. Followed by the addition of diluted methanolic extract of *K. alvarezii* to the dried cationic lipid film and the mixture was incubated at room temperature for 4 h with intermittent mixing, resulting in a final lipid concentration of 10 mM. The suspended solution was sonicated for 5 min at optimized sonication conditions to achieve a homogeneous liposome mixture, FA-conjugated PEGylated liposome was annealed for 1 h at 60 °C in a water bath and cooled to room temperature. Control liposome was formulated using the same procedure with the mixing of 100 mg [cholesterol/DSPC (45:55)] in a mixture of chloroform: methanol (2:1), followed by addition of diluted methanolic extract of *K. alvarezii*.
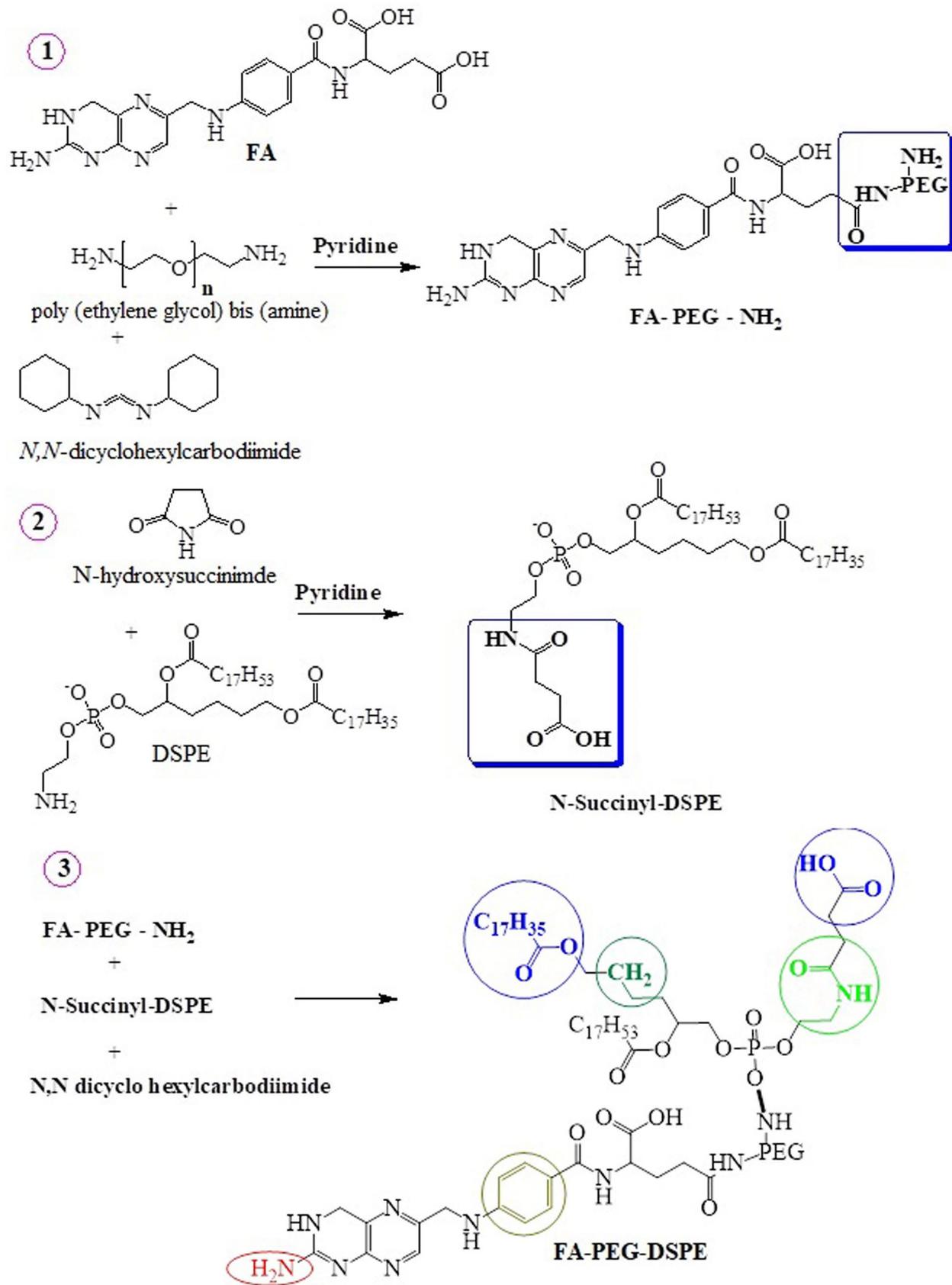
Fig. 1 Synthetic scheme of folic acid-PEG-DSPE conjugate

Determination of *K. alvarezii* extract encapsulation efficiency and loading capacity

The total concentration of *K. alvarezii* extract in the control liposome/FA-conjugated PEGylated liposome was determined using UV–Visible spectrophotometer (UV-1800 series, UV Probe 2.62 software, Shimadzu Japan) (Kunjiappan et al. 2018b). Accurately, 100 μL of control liposome/ FA-conjugated PEGylated liposome was diluted with 0.9 mL of methanol and centrifuged with 30,000 rpm for 1 h at 4 °C in a cold centrifuge. The supernatant solution containing free extract was separated and measured the absorption at 530 nm. *K. alvarezii* extract encapsulation efficiency and loading capacity were calculated by employing the following formulas:

$$\text{Loading capacity}\,(\%) = \left\{ \left[(K.\,alvarezii\ \text{extract})_{\text{added}} - (K.\,alvarezii\ \text{extract})_{\text{measured}} \right] / \text{liposome weight} \right\} \times 100. \tag{1}$$

$$\text{Encapsulation efficiency}(\%) = \left\{ \left[(K.\,alvarezii\ \text{extract})_{\text{added}} - (K.\,alvarezii\ \text{extract})_{\text{measured}} \right] / (K.\,alvarezii\ \text{extract})_{\text{added}} \right\} \times 100. \tag{2}$$

Characterization of PEGylated liposomes

The functional groups and their integrity of *K. alvarezii* extract, *K. alvarezii* extract-encapsulated liposomes (control), and FA-conjugated PEGylated liposomes were identified by FT-IR spectroscopy (Shimadzu IR Tracer-100) (Yousefi et al. 2009). A pinch of each sample ($\approx$1 mg) was mixed with an equal amount of KBr (IR grade), and a round disc was prepared using a hydraulic press. The disc was scanned with a resolution of 4 cm^{-1} in wavenumber ranges from 400 to 4000 cm^{-1}. The z-average particle size, zeta potential, size distribution of control liposome and FA-conjugated PEGylated liposome were determined by Zetasizer (Nano ZS ZEN 3600, Malvern Instruments, UK) by dynamic light scattering (DLS) method (Van Steenis et al. 2003). The physical characterization of FA-PEG-DSPE conjugate and FA-conjugated PEGylated liposomes was obtained by X-ray diffractometer (BRUKER D 8 Advance ECO XRD system equipped with SSD160 1 D Detector) (Sun et al. 2006). The operating conditions of X-ray diffractometer were as follows: targeting of Cu Kα 1 radiation ($l = 0.1542$) in a 2θ configuration with 20 keV voltage power and 30 mA current. For FE-SEM imaging to visualize the shape of FA-conjugated PEGylated liposomes, a sample solution was located on a carbon strip attached to an SEM brass; the extra solution was absorbed using sterile blotting paper and allowed to dry under a mercury lamp for 5 min. The high-resolution FE-SEM was executed by JEOL JSM6700 electron microscope (Kumar et al. 2017). Morphological details of formulated FA-conjugated PEGylated liposomes was observed under high-resolution transmission electron

microscope (HR-TEM-JEOL 2100 at an acceleration voltage of 200 kV) (Li et al. 2015). For HR-TEM imaging, few drops of freshly formulated FA-conjugated PEGylated liposomes were placed over copper grid (carbon-coated) and air dried for 5 min.

In vitro release study

In vitro *K. alvarezii* extract release from FA-conjugated PEGylated liposome was performed triplicates in 0.01 M acetate buffer solutions (pH 3.2 and 5.4) and phosphate buffer solutions 7.4 at 37 °C (Kunjiappan et al. 2019b). In detail, 5 mL of FA-conjugated PEGylated liposome was placed in dialysis bag (Molecular weight cut-off 3500 Da) incubated in a beaker containing 30 mL of buffer solutions at 37 °C and kept under shaking at 150 rpm. The buffer solution outside the dialysis bag was withdrawn at specific time intervals and replaced with fresh medium. The collected resultant supernatant was diluted with methanol and at specific time intervals, the amount of drug (*K. alvarezii* extract) released from FA-conjugated PEGylated liposome was quantified at 530 nm using UV–Visible spectrophotometry. The following formula was used for calculations:

$$\% \text{Drug release} = \left(A_0 - A_1 \right) \times 100 / A_0. \tag{3}$$

where A_0 = absorbance of the control; A_1 = absorbance of the sample.

K. alvarezii extract release kinetic studies

The above prepared *K. alvarezii* extract release data was computed using DD solver 1.0 software (Excel-plugin module) and the resultant data was fitted to the zero-order (cumulative % drug release vs. time), first-order (log % drug remaining vs. time), Higuchi (cumulative % drug release vs. square root of time), Hixson-Crowell (cube root of drug % remaining vs. time) and Korsmeyer-Peppas (log drug release vs. log time) models to verify the kinetics of drug release (Kunjiappan et al. 2019b; Dash et al. 2010). In the Korsmeyer-Peppas model, the diffusional exponent 'n' is a key indicator of the drug release kinetic mechanism from the dosage form. According to this, when "$n = 0.45$" the drug release is controlled by Fickian diffusion; when "$n = 0.89$" the drug release order corresponds to erosion mechanism/

case II transport, while "$0.45 < n > 1.0$", then the diffusional mechanism, is non-Fickian. If diffusion and drug release were found to be significant then no "n" values /kinetic data are calculated.

Stability studies

To the equivalent volume of solution (physiological buffered solutions in pH: 1.5, 3, 5, 6, 7.4 and 9; 10% NaCl and 0.5% BSA) present in a transparent glass vial, freshly prepared FA-conjugated PEGylated liposomes (approximately 1 mL) was transferred. The vial was at 37 ± 1 °C for 72 h. After 72 h, UV–Visible spectrophotometry was used to assess instantly the maximum absorbance (λ_{max}) of *K. alvarezii* extract FA-conjugated PEGylated liposomes (Bhalerao and Raje Harshal 2003).

In vitro cytotoxicity screening

The in vitro cytotoxicity of *K. alvarezii* extract FA-conjugated PEGylated liposomes in MCF-7 cells was studied using MTT colorimetric assay (Kunjiappan et al. 2018c; Lappalainen et al. 1994). In detail, cells were cultured overnight in a 96-well flat-bottom cell culture plates at a density of 1×10^5 cells/well in DMEM (100 μL) at 37 °C in 5% CO_2 atmosphere. After 24 h of initial incubation, the culture medium was replaced with fresh DMEM containing various concentrations of FA-conjugated PEGylated liposomes (200, 150, 100, 50, 25, 12.5, 6.25 μg/mL) and the cells were incubated for another 24 h. Also, negative/vehicle control and positive control (*K. alvarezii* extract) were also used for comparison. After completion of the desired treatment, the cells were washed with PBS. Next, 200 μL (5 mg mL^{-1}) of 0.5% MTT solution in serum-free medium was added to each well and incubated in 5% CO_2 at 37 °C for 4 h. Cytotoxicity was assessed by quantifying the formazan crystals converted from tetrazolium MTT salt. The medium was removed and formazan was dissolved with DMSO (100 μL). The absorbance was measured with microplate spectrophotometer (Bio-Rad, 680, Hercules, CA) at 570 nm. The following equation was used to calculate % cell viability:

$$\text{Cell viability} (\%) = At/Ac \times 100. \tag{4}$$

where, At and Ac are mean absorbance of FA-conjugated PEGylated liposomes treated and control cells, respectively ($n = 5$; where n is the number of independent experiment).

Measurement of apoptosis by AO/EB double staining method

K. alvarezii extract-encapsulated FA-conjugated PEGylated liposomes prompted cellular apoptosis was visualized by acridine orange/ethidium bromide double staining assay method (Kunjiappan et al. 2019a; Liao et al. 2018). In detail, MCF-7 cells seeded in 96-well plate at a density of 1×10^5 cells per well and incubated with 400 μL of FA-conjugated PEGylated liposome (IC_{50} value)/DMEM at 37 °C for 48 h in a humidified 5% CO_2 atmosphere. After the incubation time, cells were removed by trypsinization and suspended in 50 μL of phosphate-buffered saline (PBS), 1 μL of acridine orange (10 μg/mL in PBS) and 1 μL of ethidium bromide (10 μg/mL in PBS) for 30 min, and washed with PBS. To study the morphology of apoptotic cells, fluorescence microscopy was used. The images were captured at 40X magnification. To ensure accurate and consistent results, all the experiments were performed in triplicate.

Determination of mitochondrial transmembrane potential (ΔΨm)

The changes of mitochondrial transmembrane potential (ΔΨm) was analyzed using rhodamine-123 (cationic fluorophore) by the previously described method (Kunjiappan et al. 2019a; Biswas et al. 2012). In detail, cells (MCF-7) were cultured at 37 °C for 4 h with IC_{50} concentration of FA-conjugated PEGylated liposomes and the cells were rinsed with ice-cold PBS. Then, cells were stained with 2 μM rhodamine-123 and incubated at 37 °C in the dark for 30 min. Next, the cells were washed twice and fluorescence intensity was calculated at 480 nm (excitation wavelength) and 530 nm (emission wavelength) using Spectramax M2 fluorescence spectrophotometer (Molecular Devices, USA). The reduced transmembrane potential of mitochondria was indicated by the reduction in staining of rhodamine 123.

4′,6′-diamino-2-phenylindole. 2HCl (DAPI) fluorescent staining for nuclear morphology study

The morphological changes of nuclear materials were assessed after staining with DAPI (Kunjiappan et al. 2019a; Wang et al. 2018). In brief, MCF-7 cells (1×10^5 cells/well density) were seeded onto a coverslip of 24-well flat-bottom microplate and maintained at 37 °C in a CO_2 incubator for overnight. Cultured cells were treated with IC_{50} concentration of FA-conjugated PEGylated liposomes and incubated at 37 °C for 48 h. The cells were subsequently washed twice with $1 \times$ PBS and fixed with 4% paraformaldehyde solution for 30 min. Fixed cells were incubated with 20 μL (0.1 μg/mL) of DAPI in the dark at room temperature for 5 min; then cells were washed twice with PBS and examined under fluorescent microscope (Labomed LX-400, Binocular Fluorescence Compound Microscope). The number of apoptotic

cells was evaluated in representative fields and percentage of apoptotic cells were calculated.

Determination of intracellular ROS (reactive oxygen species) levels

Intracellular generation of ROS in control and treated breast cancer cells (MCF-7 cells) were determined using the fluorescent dye (DCFH-DA) (Kunjiappan et al. 2015; Gijsens et al. 2002). In detail, MCF-7 cells (1×10^5 cells/well) seeded in 24-well culture plate and incubated for 24 h. Cells were then exposed with 10% FBS supplemented with IC_{50} concentration of FA-conjugated PEGylated liposomes for 24 and 48 h further incubation. The time was selected to give adequate amounts of drug uptake within a time frame in which ROS generation may be projected. Later, cells were washed twice with $1 \times PBS$ and labelled with 20 µM DCFH-DA for 15 min at 37 °C. Next, the cells were placed on ice, filtered using cell strainer (70 µM) and the reaction mixture was exchanged to PBS (200 µL) with subsequent 10 min incubation in the dark at room temperature. The fluorescence intensity change was monitored at 475 nm (λ_{ex}) and 525 nm (λ_{em}) using Spectramax M2 fluorescence spectrophotometer (Molecular Devices, USA).

Statistical analysis

The experimental data were analyzed using Statistical Package for Social Science (SPSS) version 20.0 software (SPSS Inc., Chicago, IL, USA). All studies were repeated at least three times. Obtained quantitative data were expressed as mean ± standard deviation. One-way ANOVA and Dunnett's multiple comparison method is used to study the significance of the statistical method. A p value < 0.05 was considered to indicate a statistically significant difference. For cytotoxicity studies, from the % viability values, IC_{50} was calculated using robust curve fit non-linear regression method. ROS generation data was analyzed using a paired t-test method.

Results

K. alvarezii crude extract

Figure 2 shows FT-IR spectrum of *K. alvarezii* methanolic extract to confirm the functional groups. The characteristic spectrum showed O–H stretching of carboxyl groups (3338 cm^{-1}), –CH$_2$ stretching of aliphatic groups (2922 and 2848 cm^{-1}), alkynyl C–H stretching (2353 cm^{-1}), alkenyl C=C stretching (1637 cm^{-1}), vinyl C–H in-plane bending (1406 cm^{-1}), methylene C–H bending (1217 cm^{-1}), trans C–H out of plane (952 cm^{-1}) and cis C–H out of plane bending (719 cm^{-1}). From GC–MS [Supplementary Fig. 1 (a)]
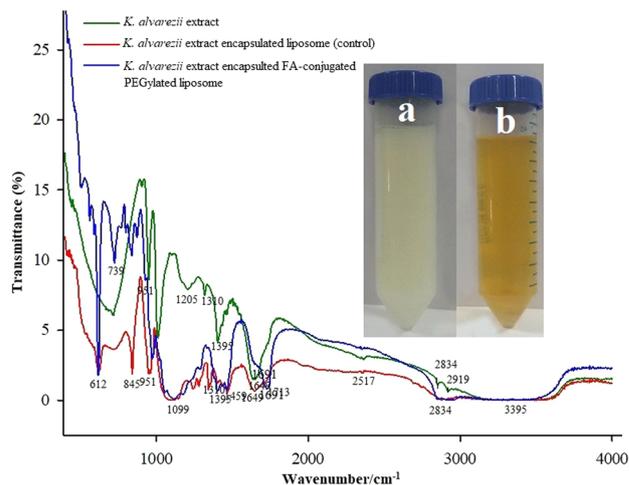
Fig. 2 FT-IR spectra of *K. alvarezii* extract, *K. alvarezii* extract-encapsulated PEGylate liposome, *K. alvarezii* extract-encapsulated FA-conjugated PEGylate liposome
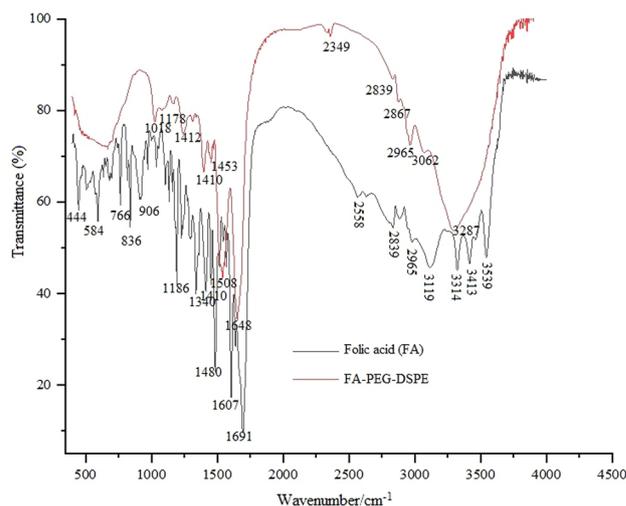
Fig. 3 FT-IR spectra of FA and folic acid-PEG-DSPE conjugate

analysis of *K. alvarezii* extract showed 15 valued bioactive compounds (listed in Supplementary Table 1). Supplementary Fig. 1 (b) shows the RP-HPLC spectra of *K. alvarezii* extract. Four peaks were detected and identified as compound -1 (3-hydroxy benzoic acid), compound-2 (Cinnamic acid), compound-3 (Chlorogenic acid) and compound-4 (Gallic acid) (Baskararaj et al. 2019).

FA-PEG-DSPE conjugate

Using TLC grade silica gel GF (75:36:6 chloroform/methanol/water) showed a new spot ($R_f = 0.54$) due to the formation of the product (FA-PEG-NH$_2$). The appearance of –NH ($R_f = 0.72$) from the reaction mixture was confirmed

by ninhydrin spray. The FT-IR spectra of FA and FA-PEG-DSPE conjugates are depicted in Fig. 3. Absorbance peaks at 1453 and 1508 cm^{-1} are related to aromatic C=C stretching vibrations in folicacid (FA). FA-PEG-DSPE conjugate spectrum shows two remarkable absorption peaks at 1691 cm^{-1} due to the presence of amide (–NH) group and 1648 cm^{-1} due to the presence of ester (–COO) group of DSPE. These absorption peaks indicated that FA had been structurally transferred into FA-PEG-DSPE. Moreover, a sharp peak at 1178 cm^{-1} is representing to P=O stretching vibrations in DSPE. The peaks at 2867 and 2965 cm^{-1} are related to C–H stretching bands in the aliphatic structure of PEG, FA and DSPE. The broadband at 3287 cm^{-1} is recognized to O–H acid groups and O–H on the ring of folicacid. The ^{1}H-NMR (Fig. 4) analysis of the new formulated compound is under the assigned structures. The ^{1}H-NMR (δ: ppm) spectrum of FA-PEG-DSPE showed respective peaks of aliphatic CH$_2$ group at 1.4. The δ value of 2.8 confirms the presence of –NH$_2$, further aromatic, amide, carboxylic acid and ester δ signals are observed at the respective peak area. The observed peak of the corresponding groups provides a piece of strong evidence for the formation of the formulated structure FA-PEG-DSPE.

Characterization of PEGylated liposomes

K. alvarezii extract was encapsulated in cholesterol/DSPC and FA-PEG-DSPE/cholesterol/DSPC named as control and FA-conjugated PEGylated liposomes, respectively. The encapsulation efficiency and loading capacity of *K. alvarezii* extract in control and FA-conjugated PEGylated liposomes were detected to be 84.56%, 82.72% and 13.42%, 12.81%, respectively. The FT-IR spectra of freeze-dried samples of control and FA-conjugated PEGylated liposomes are displayed in Fig. 2 [insert control liposome Fig(a) and FA-conjugated PEGylated liposome Fig(b)]. The FT-IR spectra of

K. alvarezii extract–encapsulated FA-conjugated PEGylated liposomes showed strong absorption peak at 3395 cm^{-1} due to O–H group of active polyphenolic compounds of *K. alvarezii* extract, carboxyl moiety of FA. The absorption peak at 2834 cm^{-1} confirms the presence of C-H stretching bands in the aliphatic structure of PEG, FA and DSPE. The peak at 1713 cm^{-1} indicates the stretching vibration of benzene ring skeleton of FA and polyphenolic compounds of *K. alvarezii* extract. While, the amide (–NH) group and ester (COO) group of conjugate DSPE are confirmed by the presence of peak at 1649 cm^{-1} and 1691 cm^{-1}, respectively. A peak at 1099 cm^{-1} represents C-O stretching of α–anomer of polyphenolic compounds of *K. alvarezii* extract and FA. The peak at 2834 cm^{-1} is related to C–H stretching band in the aliphatic structure of the PEG, FA and DSPE. In Fig. 5, the XRD crystalline peaks of FA-PEG-DSPE was absent in the XRD pattern of *K. alvarezii* extract–encapsulated
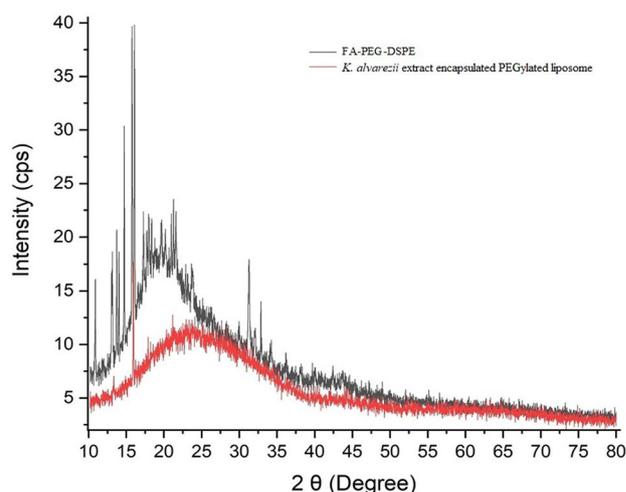
Fig. 5 XRD pattern of folic acid-PEG-DSPE conjugate and *K. alvarezii* extract-encapsulated FA-conjugated PEGylate liposome
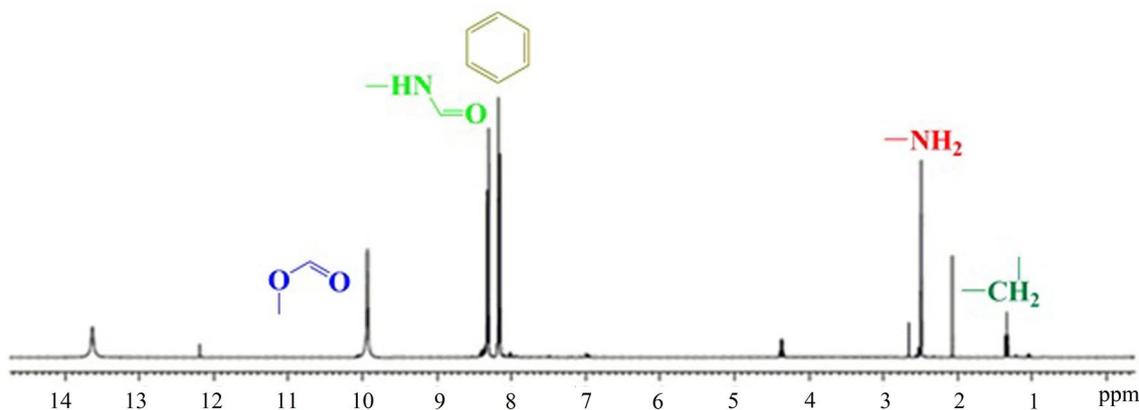
Fig. 4 Proton magnetic resonance spectrum of Folic acid-PEG-DSPE conjugate

FA-conjugated PEGylated liposomes. This spectacle may be demonstrated to the possible interaction such as hydrogen bonding between polyphenolic compounds of *K. alvarezii* extract and FA-PEG-DSPE. The intensity weighted mean diameter (z average), zeta potential of the *K. alvarezii* extract-encapsulated control and FA-conjugated PEGylated liposomes were measured using DLS and are displayed in Fig. 6 (a–d) respectively. The mean diameter of *K. alvarezii* extract-encapsulated control and FA-conjugated PEGylated liposomes was found to be 110 ± 6 nm and 140 ± 5 nm, respectively. The observed zeta potential of $- 5$ mV and $+ 0.2$ mV and polydispersity index was 0.25 ± 0.014

and 0.48 ± 0.026, respectively. These reports indicated that FA-conjugated PEGylated liposomes are monodispersed and highly stable. FESEM images (Fig. 7a, b) revealed that *K. alvarezii* extract-encapsulated FA-conjugated PEGylated liposomes were found to be smaller spherical particles with ~ 140 nm size. Further, TEM images (Fig. 8) showed that the diameter of *K. alvarezii* extract-encapsulated FA-conjugated PEGylated liposomes were ranged from 100 to 160 nm and the liposomes are spherical in shape.
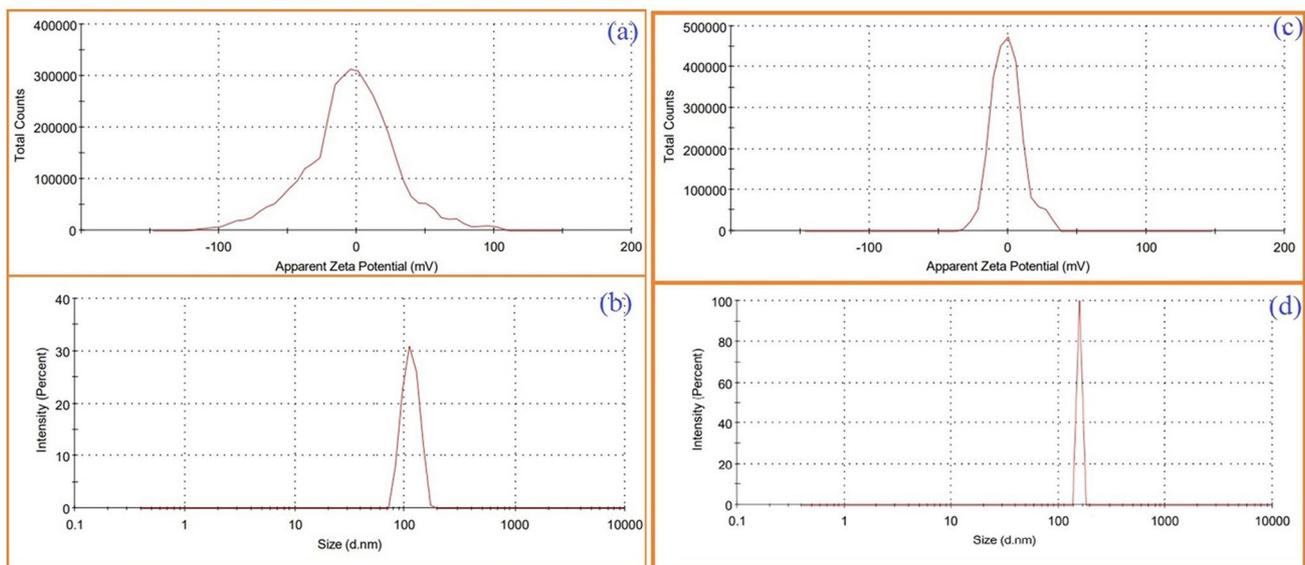
Fig. 6 The DLS measurement of average particle size of *K. alvarezii* extract-encapsulated PEGylate liposome (control) (**a**); Zeta potential of *K. alvarezii* extract-encapsulated PEGylate liposome (control) (**b**); average particle size of *K. alvarezii* extract-encapsulated FA-conjugated PEGylate liposome (**c**); Zeta potential of *K. alvarezii* extract-encapsulated FA-conjugated PEGylate liposome (**d**)
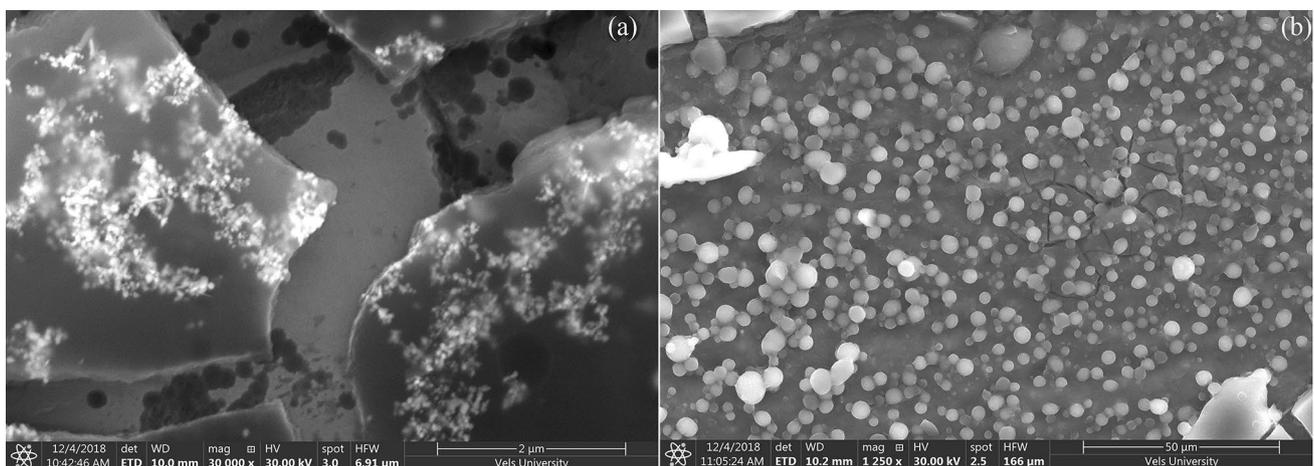
Fig. 7 FE-SEM images of *K. alvarezii* extract-encapsulated FA-conjugated PEGylate liposome
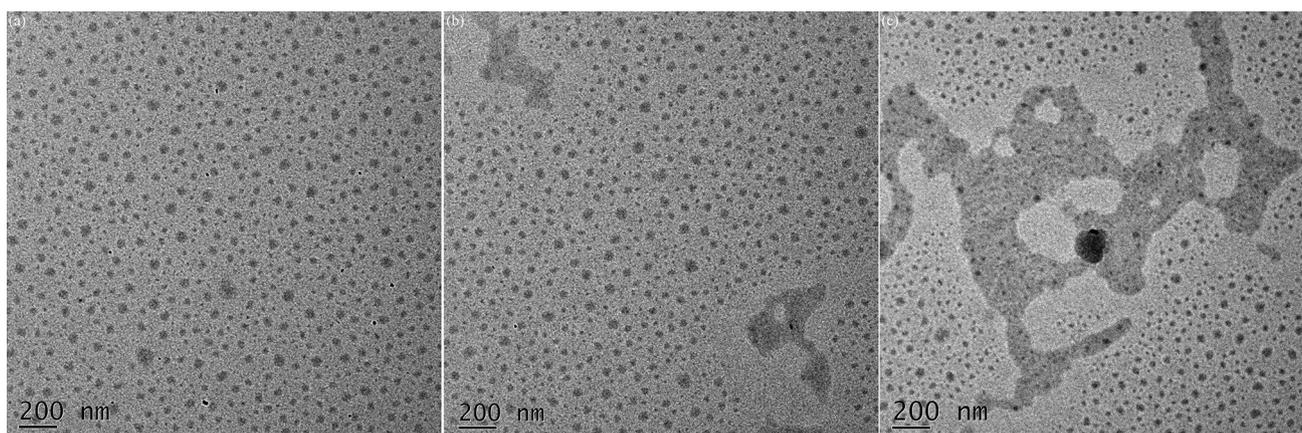
Fig. 8 TEM images of *K. alvarezii* extract-encapsulated FA-conjugated PEGylate liposome
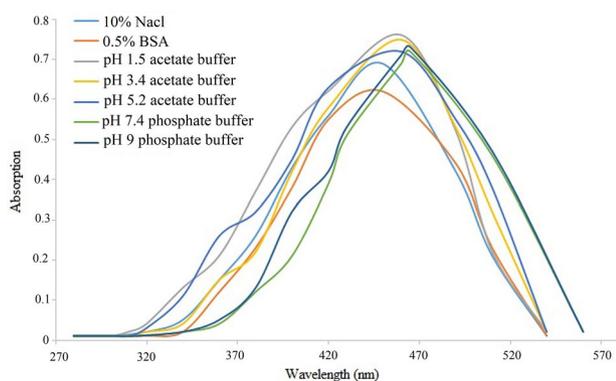
Fig. 9 The in vitro stability studies of *K. alvarezii* extract-encapsulated FA-conjugated PEGylate liposome in different physiological medium and pH buffer solutions. A stable peak appeared for 10% NaCl, 0.5% BSA and physiological buffered solutions (pH: 1.5, 3.4, 5.2, 7.4 and 9), between the range of 460 nm and 460–465 nm, respectively

Fig. 10 In vitro *K. alvarezii* extract release pattern of FA-conjugated PEGylate liposome in pH 3.2, 5.4 and pH 7.4 at 37 ºC in PBS buffer as a function of time. Data were represented as mean ± standard deviation ($n = 3$)

Stability studies

Chemical stability is one of the prime parameters for the storage of pharmaceutical formulations. Figure 9 demonstrates the stability of freshly formulated *K. alvarezii* extract-encapsulated FA-conjugated PEGylated liposomes in 10% NaCl (w/v), 0.5% BSA (w/v), physiological buffer solutions (pH: 1.5, 3.4, 5.2, 7.4 and 9). The λ_{max} of *K. alvarezii* extract-encapsulated PEGylated liposomes in 10% NaCl (w/v), 0.5% BSA (w/v) were found 450 nm and physiological buffer solutions (pH: 1.5, 3.4, 5.2, 7.4 and 9) were found to be 460–465 nm. At pH 7.4 phosphate and 5.4 in acetate-buffered medium, *K. alvarezii*

extract-encapsulated PEGylated liposome displayed about 5 nm shifts in its λ_{max}. These data demonstrated the excellent stability of *K. alvarezii* extract-encapsulated PEGylated liposomes at various conditions.

Drug release studies

Figure 10 demonstrates the release profile of *K. alvarezii* extract from PEGylated liposomes in 0.01 M acetate buffer system (pH 3.2 and 5.4) phosphate buffer solution pH 7.4 at 37 °C. The release profile was exposed as a cumulative percentage of the released *K. alvarezii* extract in time. An authenticated UV–Visible spectrophotometry was used to measure the quantity of *K. alvarezii* extract released. It can be observed that the release of *K. alvarezii* extract from PEGylated liposomes was in slow, steady and sustained

release manner, which is pH-dependent and higher amount of *K. alvarezii* extract was released at pH 5.4. The cumulative release of *K. alvarezii* extract from PEGylated liposome for first 30 min was found to be $0.08 \pm 0.0006\%$ (pH 3.2), $0.08 \pm 0.0007\%$ (pH 5.4) and $0.08 \pm 0.0007\%$ (pH 7.4). After 18 h, approx. 18% (pH 3.2), 21% (pH 5.4) and 18% (pH 7.4) of *K. alvarezii* extract was released from PEGylated liposomes with gradual increase. The variations in pH did not significantly affect the *K. alvarezii* extract release from PEGylated liposomes. After, a steady-state increase in accumulative amount and release rate of *K. alvarezii* extract released from PEGylated liposomes was observed (at pH 3.2, 5.4 and 7.4 release rate was found to be 70.47%, 81.35%, and 73.72%, respectively) after 66 h. The observed experimental data exposed that *K. alvarezii* extract release from PEGylated liposome was higher and efficient at pH 5.4 compared to neutral pH 7.4.

Drug release kinetics

Additionally, the drug release kinetics of *K. alvarezii* extract release from PEGylated liposomes was determined using the above drug release data. The estimated drug release data were fitted into various kinetic models, including zero order, first order, Higuchi, Korsmeyer-Peppas and Hixson-Crowell models. The summary of in vitro drug release kinetics data was presented in Table 1. For each kinetic model, the regression coefficient (r^2) value was generated and the release rate constant of these models was also predicted. In general, the closer r^2 value is to 1 the better the fit. The first-order kinetics regression coefficient (r^2) values are higher than that of zero-order kinetics i.e., 0.9616–0.9001 (in pH 3.2), 0.9692–0.9285 (in pH 5.4) and 0.9618–0.8961 (in pH 7.4). These values are very close to 1, hence these models were considered to be good fit. The data was most fitted to the Higuchi model, with a regression coefficient (r^2) of 0.8824 (in pH 3.2), 0.8878 (in pH 5.4) and 0.8848 (in pH 7.4). According to this model, the PBS solution penetrates the lipid vesicle and dissolves the entrapped *K. alvarezii* extract and so the *K. alvarezii* extract release seems to be a process majorly controlled by diffusion. In addition, the diffusion exponent (n) in Korsmeyer-Peppas model was slightly varied [0.742 (pH 3.2), 0.778 (pH 5.4) and 0.733 (pH 7.4)]. This also demonstrates the uniform dissolution and controlled release of the formulation. Further, the observed release kinetics data indicates the non-Fickian behaviour of *K. alvarezii* extract-encapsulated PEGylated liposomes formulation. In Hixon Crowell model, high r^2 values (0.9741) indicated a fixed amount of drug release and uniform dissolution from the PEGylated liposomes. However, the release of *K. alvarezii* extract from PEGylated liposomes was principally controlled as well as sustained at fixed quantity of drug release pattern at pH 3.2, 5.4 and 7.4.

Table 1 Drug release kinetics profile of *K. alvarezii* extract-encapsulated PEGylated liposome

Model	Parameter	*K. alvarezii* extract from PEGylated liposome		
		pH 3.2	pH 5.4	pH 7.4
Zero order $F = K_0 \times t$	K_0	0.015	0.017	0.015
	r^2 Adjusted	0.9001	0.9285	0.8961
	AIC	340.521	337.430	343.741
First order $F = 100 \times [1\text{-Exp}(-k1 \times t)]$	K_1	0.01	0.01	0.01
	r^2 Adjusted	0.9616	0.9692	0.9618
	AIC	300.411	302.144	301.786
Higuchi model $F = KH \times t1/2$	K_h	0.904	1.026	0.926
	r^2 Adjusted	0.8824	0.8878	0.8848
	AIC	347.390	356.379	348.114
Korsmeyer-Peppas model $F = kKP \times t^n$	kKP	0.1272	0.1078	0.140
	r^2 Adjusted	0.9363	0.9535	0.9356
	n	0.742	0.778	0.733
	AIC	323.637	321.364	325.669
Hixon-Crowell model $F = 100 \times [1-(1-kHC \times t)^3]$	kHC	0.001	0.001	0.001
	r^2 Adjusted	0.9554	0.9741	0.9555
	AIC	306.618	294.757	308.127

Where, *AIC* akaike information criterion, *F* fraction of drug release in time *t*, K_0 apparent rate constant of zero-order release constant, K_1 first-order release constant, K_H higuchi constant, *kKP* Korsmeyer–Peppas rate constant, *kHC* Hixon–Crowell constant, *n* diffusional exponent. And r^2 squared correlation coefficient

Cytotoxicity studies

The potential cytotoxicity of *K. alvarezii* extract-encapsulated PEGylated liposomes was determined by MTT assay on MCF-7 cancer cells. It was found that *K. alvarezii* extract-encapsulated PEGylated liposomes exerts quantifiable cytotoxicity of cells in a concentration-dependent manner, as shown in Fig. 11a. For 6.25 μg/mL concentration of *K. alvarezii* extract-encapsulated PEGylated liposomes concentration, no statistically significant change of viability (98%) was observed, whereas, 100 μg/mL concentration of *K. alvarezii* extract-encapsulated PEGylated liposomes showed 43% of cellular viability. About 82% cellular viability was observed with 100 μg/mL concentration of *K. alvarezii* extract and 28% of cell viability was observed with 100 μg/mL of doxorubicin. Moreover, 50% of cell viability was observed at 81 μg/mL *K. alvarezii* extract-encapsulated PEGylated liposomes and this concentration was selected as half-maximal inhibitory concentration (IC_{50}) of *K. alvarezii* extract-encapsulated PEGylated liposomes for further study. After incubation with IC_{50} concentration (81 μg/mL) of *K. alvarezii* extract-encapsulated PEGylated liposomes,

the morphology of MCF-7 cells has changed as depicted in Fig. 11 (b, c).

Apoptosis analyses

The morphological changes induced by 81 μg/mL of *K. alvarezii* extract-encapsulated PEGylated liposomes (IC_{50} concentration) in MCF-7 cancer cells are analyzed by acridine orange (AO)/ethidium bromide (EB) double staining assay method. The (AO)/(EB) double staining principle combines the differential uptake of fluorescent DNA binding dyes (AO/EB) and also the morphological changes of chromatin condensation within the stained nucleus. The AO/EB assay is suitable for *K. alvarezii* extract-encapsulated PEGylated liposomes allowing to their cell membrane disruption potential. After 48 h of exposure with 81 μg/mL of *K. alvarezii* extract-encapsulated PEGylated liposomes, the cells are harvested, stained with AO/EB and visualized in a fluorescent microscope. In negative control cells, no significant apoptosis was observed (Fig. 12a). In contrast, in the *K. alvarezii* extract-encapsulated PEGylated liposomes treated cells round, irregular shape with condensed nuclei, distorted cell membrane and the presence of apoptotic bodies were
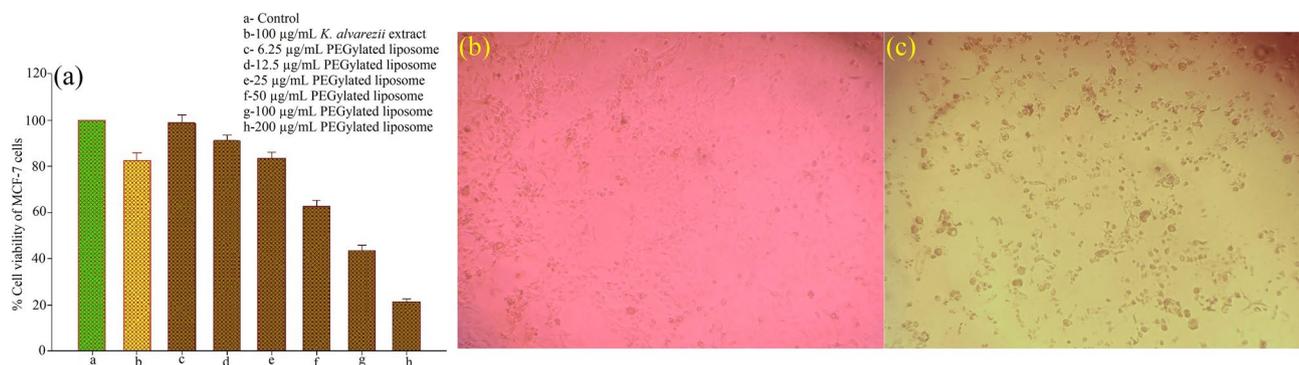
Fig. 11 Cytotoxic activity of human adenoma breast cancer (MCF-7) cells using different concentrations of *K. alvarezii* extract-encapsulated FA-conjugated PEGylate liposome after 24 h treatment. The percentage of apoptotic cells increased dose dependently. Values are mean ± standard deviation of triplicate measurements ($p < 0.05$) (**a**); Morphology of the control cells (**b**); and treated cells (**c**) observed using a phase-contrast microscope

Fig. 12 Apoptotic morphological variations of MCF-7 cells identified with AO/EB staining and observed using fluorescence microscope (**a**) control cells; (**b**) 81 μg/mL of *K. alvarezii* extract-encapsulated FA-conjugated PEGylate liposome for 48 h
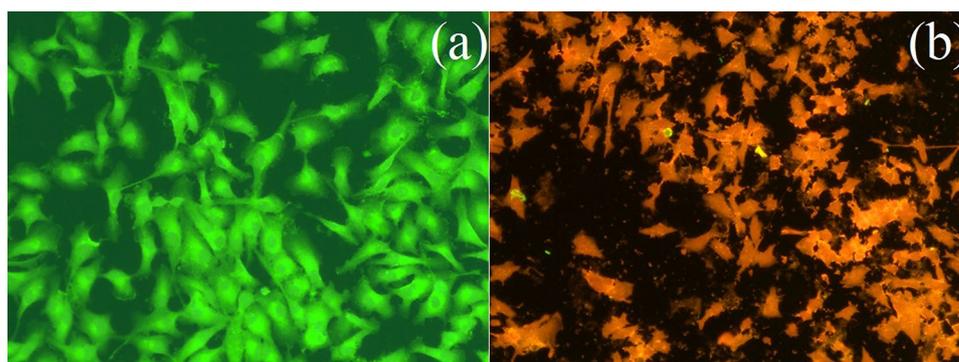
Fig. 13 Effects of *K. alvarezii* extract-encapsulated FA-conjugated PEGylate liposome on mitochondrial transmembrane potential in MCF-7 cancer cells. Control cells (**a**); notable loss of mitochondrial transmembrane potential on treated cells (**b**)
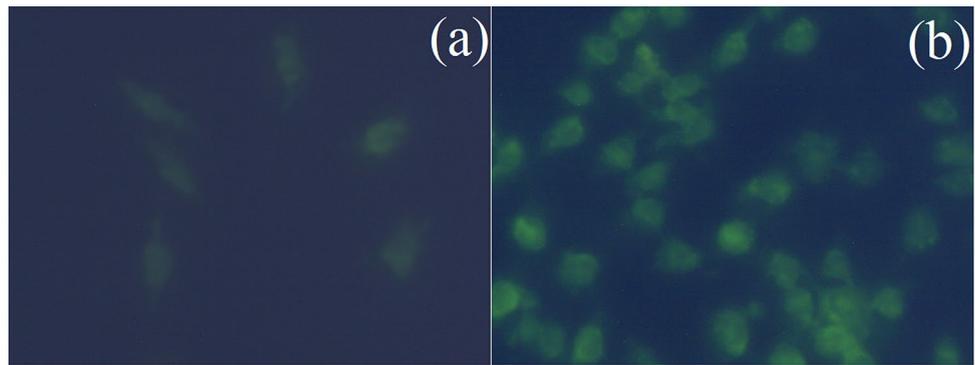
Fig. 14 DAPI stained image of MCF-7 cancer cells. Control cells (**a**) and (**b**) treatment with *K. alvarezii* extract-encapsulated FA-conjugated PEGylate liposome. Chromatin fragmentation is shown with arrow
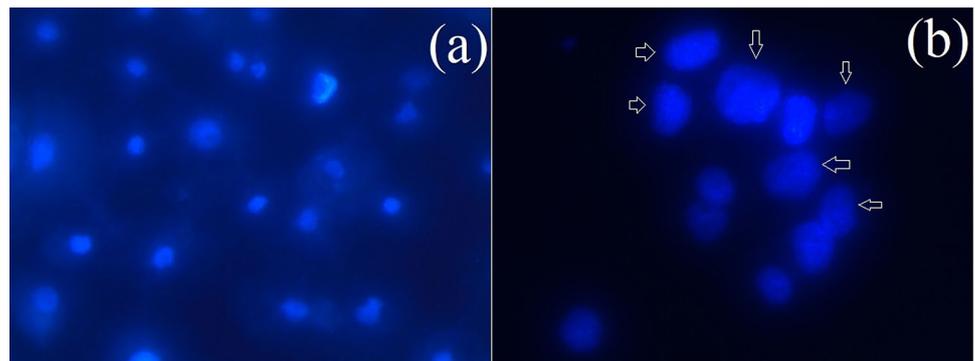
observed (Fig. 12b). This result indicated the high concentration of *K. alvarezii* extract entered into the MCF-7 cancer cells.

Mitochondrial transmembrane potential (ΔΨm)

To determine the mitochondrial transmembrane collapse, MCF-7 cancer cells were stained with rhodamine-123 after treated with *K. alvarezii* extract-encapsulated PEGylated liposomes. In the MCF-7 cells, after exposure with 81 µg/mL of *K. alvarezii* extract-encapsulated PEGylated liposomes, a significant mitochondrial membrane potential loss was observed (Fig. 13a, b). Besides, *K. alvarezii* extract-encapsulated PEGylated liposomes induced depolarization of the mitochondrial membrane as well. Our results demonstrated that the *K. alvarezii* extract-encapsulated PEGylated liposomes permeate mitochondrial membrane via endocytosis and leads to cell death (Fig. 14).

4′,6′-diamidino-2-phenylindole.2HCl (DAPI) fluorescent staining

DAPI staining was assessed to distinguish the potential nuclear changes like DNA damage which are accountable for the cellular inhibitory effect of *K. alvarezii* extract-encapsulated PEGylated liposomes related to the induction
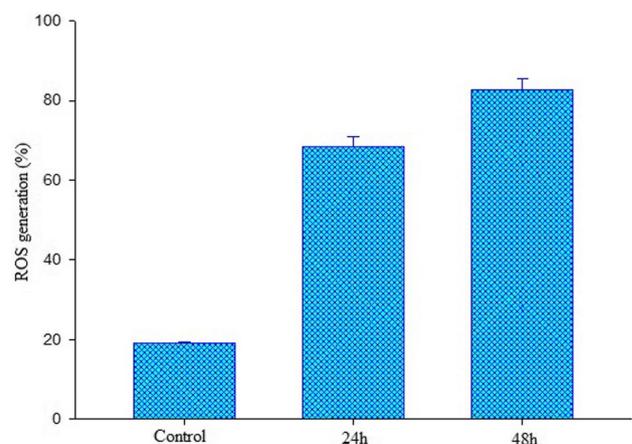
Fig. 15 Effects of 81 µg/mL of Rt encapsulated *K. alvarezii* extract-encapsulated FA-conjugated PEGylate liposome on ROS generation (percentage of control value) in MCF-7 cancer cells. Results expressed as mean ± standard deviation triplicate measurements ($p < 0.05$)

of cell apoptosis. Figure 14a, b represented the morphology of DAPI stained MCF-7 cell lines without (control) and treated *K. alvarezii* extract-encapsulated PEGylated liposomes (24 h), respectively. The collection of cells (Fig. 14a) treated with 81 µg/mL of *K. alvarezii* extract-encapsulated PEGylated liposomes exhibited typical apoptotic morphology with cell shrinkage, nuclear fragmentation

and DNA condensation. Using DAPI staining, the intact nuclear morphology in the negative control collection of cells was observed.

ROS generation assay

Figure 15 shows the significantly increased level of intracellular ROS in MCF-7 cancer cells treated with IC_{50} concentration (81 µg/mL) of *K. alvarezii* extract-encapsulated PEGylated liposomes as compared to untreated control cells.

Discussion

Breast cancer has become one of the highest incidences of malignant tumor in the global women society (Bray et al. 2018). Conventional chemotherapy has non-targeted distribution and leads to severe toxicity, less bio-availability at disease site and permanently fails in MDR (Jain 2017). The natural bioactive compounds are frequently considered due to cost-effective, better bio-compatibility and productive comparable anti-cancer activity with limited toxicity than synthetic compounds (McClements et al. 2009). A majority of bioactive compounds were highly insoluble/soluble in water and they might be speedy hepatic first-pass metabolism, the metabolites are less active/toxic effects and do not reach disease site (Shimizu 1985; Hidalgo et al. 2018). Bio-availability is one of the critical parameters ensuring the bio-efficacy of bioactive compounds for pharmaceutical formulations (Becker et al. 2011). Presently, some efforts have been taken on the cationic lipid vehicle entrapped with natural bioactive compounds with higher bio-availability and targeted efficiency without affecting normal healthy cells. Here, PEGylated liposomes were formulated and their surface was modified with folic acid for effective targeted delivery. The bioactive compounds of *K. alvarezii* crude extract were encapsulated with PEGylated liposomes and its effect against cancer progression in vitro was studied with MCF–7 cell lines. The apoptosis effect of *K. alvarezii* crude extract was proven with DAPI, acridine orange/ethidium bromide double staining, ROS and mitochondrial membrane leakage methods.

Marine algae are rich sources of therapeutics; among, seaweeds are considered as valuable sources of protein, iodine, vitamin, minerals and their metabolites has been proven for their promising activity against cancer incidences (Yaakob et al. 2014; Sithranga Boopathy and Kathiresan 2010). There have been many reports available on antioxidant, anticancer and immunomodulating activities of seaweeds (Jiménez Escrig et al. 2001). *K. alvarezii* extracts were found to be suitable for their therapeutic properties and their presence is rich in nutrients and nutraceuticals (Kumar et al. 2008). The extracts of *K. alvarezii* has been considered as antioxidant,

antiviral and anticancer compounds (Ferraces-Casais et al. 2012). *K. alvarezii* was collected, and active metabolites were extracted through microwave-assisted extraction (MAE) with minimal consumption of methanol (Baskararaj et al. 2019). Several scientific studies accounted for the advantages and applicability of microwave-assisted extraction upon medicinal plants. Carrageenan was extracted from *Hypnea musciformis*, well-known red algae (Ghannam et al. 2013). The authors accounted that MAE is a rapid method to extract metabolites than conventional methods; also, MAE can be applied under low availability of algae powder with maximum cropping of bioactive compounds (Ganesan et al. 2018).

Liposomes are potential drug carriers, having the capability of delivering drugs across cell membrane provided with stability and bioavailability; also, liposomes can protect the molecules loaded in its core from digestion (Torchilin 2005). Liposomes were fabricated with FA-PEG-DSPE / cholesterol / DSPC composition and *K. alvarezii* methanolic extract was encapsulated in its core by thin-film hydration technique. The liposomes were characterized for its entrapment and loading efficiency. Entrapment efficiency, size distribution and bioavailability of liposomes are based on the methodology employed to fabricate liposomes. Thin-film hydration is one of the widely utilized and most straight forward methods of fabricating liposomes (Solis-Gonzalez 2014). Đorđević et al. (2015) accounted that the size of the liposomes formulated by thin-film method depends on the bilayer composition and a load of molecules in its inner core. Hydroxyzine and Cetirizine-loaded liposomes were formulated using thin-film hydration and freeze-thawing method by Elzainy et al. (2005). The authors analyzed the long term stability of liposomes by varying the duration of hydration of thin lipid film, freeze-thawing treatments and pH values. The results concluded that the liposomes synthesized with thin-film hydration method provided stability to liposomes for long term storage.

Even though liposomes are being considered as promising agents for delivering materials intracellular, they can be degraded by proteolytic enzymes, rapidly cleared by the reticuloendothelial system and can induce opsonisation process which ultimately leads to reducing half-life under peripheral circulating system (Prokop and Davidson 2008). PEGylation, the process in which polyethylene glycol chains are embedded to outer surface of liposomes can overcome these shortcomings and can improve pharmacokinetics of liposomes in the bloodstream (Harris and Chess 2003). PEGylated liposomes surface was conjugated with folic acid to enhance bioavailability and for folate receptor (naturally overexpressed on the surface of breast cancer cells) targeted delivery. PEGylation of liposomes for enhancement of extended circulation was accounted by numerous research reports (Gabizon 2001). Folate receptor targeted

liposomal nanoparticles were fabricated for efficient delivery with the target of chemoresistant breast cancer cells. The efficacy of folate receptor-targeted liposomal nanoparticles was proved with various in vitro and in vivo experiments. The same research group has previously reported that folic acid conjugated keratin nanoparticles encapsulated with rutin were non-covalently binded on the membrane surface folate receptor of breast cancer cells (MCF-7) (Kunjiappan et al. 2019a). Its folate conjugation was broken and keratin nanoparticles were subjected to smooth endocytosis on the cancer cells. The authors also accounted that the nanomaterial was effective against doxorubicin-resistant tumors; also, increase in tumor selectivity enhances the therapeutic outcome of the liposomes (Riganti et al. 2011). Cationic lipid type folate acid-modified PEGylated liposomes were fabricated for the delivery of siRNA in tumor cells. The results revealed that the FA-PEG modified cationic liposomes boosted in vitro gene silencing activity when compared to unmodified liposomes (Hattori et al. 2019).

In a pathophysiological state, the physicochemical properties like stability, size, shape, physical nature, the zeta potential of the liposomes are essential parameters for determining its drug delivery applications. Large size liposomes (μM) allow to carry macromolecules (like enzymes, proteins) but are more rapidly eliminated from the blood circulation by mononuclear phagocyte system, while small size (nm) liposomes limit the size of particles but increases the half-life circulation. Under observed with FE-SEM and TEM, the formulated *K. alvarezii* extract-encapsulated PEGylated liposomes were 140 nm in diameter with majorly spherical shape, which was verified with DLS reports. Also, the spherical shape of the liposomes instigated EPR effect which resulted in the initiation of the cancer cells nuclear materials leak. This was one of the significant advantages in lipid-based drug delivery system. The X-ray diffraction analysis established that the formulated *K. alvarezii* extract-encapsulated PEGylated liposomes are monodispersed, amorphous in nature and they readily bind to the target receptor and then release the active drug at targeted cells. Zeta potential is one of the critical criteria for the stability of liposomes in the colloidal state. Liposomes with surface charge in terms of zeta potential are more rapidly uptaken into cancer cells and can release the intended bioactive compounds. The formulated *K. alvarezii* extract-encapsulated PEGylated liposomes were displayed high stability in 10% NaCl, 0.5% BSA and at various pH buffer solutions. The observed higher stability of *K. alvarezii* extract-encapsulated PEGylated liposomes formulation might be responsible for controlled and sustained release of *K. alvarezii* extract from PEGylated liposomes.

Followed by the physicochemical characterization, in vitro release of *K. alvarezii* extract from PEGylated liposomes was studied in various pH buffer solution to (a) authorize the successful encapsulation of *K. alvarezii* extract, (b) study the *K. alvarezii* extract release kinetics and release mechanism from PEGylated liposomes, (c) find out the most favourable conditions (pH) for maximal release of *K. alvarezii* extract from PEGylated liposomes, which is necessary for further extended in vivo studies. In this work, the observed *K. alvarezii* extract release data was extrapolated by five models (zero-order, first-order, Higuchi, Korsmeyer-Peppas and Hixson-Crowell models) to know the mechanism of *K. alvarezii* extract release from this formulation. The observed regression coefficient (r^2) for each release model was tabulated in Table 1. Based on the above results, it was found that the highest content, *K. alvarezii* extract (81.35%) was released from liposomes at pH 5.4 (acidic medium). Compared to healthy tissues, solid tumor tissues are more acidic (pH: 5–6). In this study, we observed that formulated liposomes at pH 5.4 medium mimicking tumor microenvironment, facilitates *K. alvarezii* extract release from PEGylated liposomes. Moreover, in vitro release profiles of *K. alvarezii* extract from all this formulation might be best expressed by Korsmeyer-Peppas equation, as the plots showed the highest regression coefficient ($r^2 = 0.93$ to 0.95). The 'n' value was applied to specify Fickian and non-Fickian diffusion. For spherical liposomes, $n \leq 0.43$ signifies case I transport (Fickian release), while $n = 0.85$ signifies controlled delivery (case II transport). Intermediate values, i.e. $0.43 < n < 0.85$, describes a non-Fickian release (an anomalous behaviour corresponding to coupled diffusion/polymer relaxation). In our study, at pH 5.4, n value was > 0.778. Hence, the drug release follows non-Fickian diffusion kinetics and zero-order kinetics.

Viability of breast cancer cells against *K. alvarezii* extract-encapsulated PEGylated liposomes was assessed with MTT assay. The potential inhibitory concentration of *K. alvarezii* extract-encapsulated PEGylated liposomes against cancer cells (in vitro) was found to be 81 μg/mL. The role of *K. alvarezii* extract on controlling cancer progression was proven with different types of cancer models, including mammary, cervical and colon. *K. alvarezii* extract was studied against mammary cancer in vitro with MCF-7 cell lines and 4.100 ± 0.690 mg/mL of extract reported as potential concentration to inhibit the progression of cells up to 50%. Further, the same was proven in Sprague–Dawley rat models (Chang et al. 2017). Prevention of colon carcinogenesis was proven with HCT116 cell lines in vitro with low molecular weight κ-Carrageenan, an extract of *K. alvarezii* at 1000 μg/ml. The results accounted that the extracts having the capability of inducing apoptosis and it was proven with flow-cytometry cell cycle analysis (Annamalai et al. 2015). These reports support our findings that the extracts of *K. alvarezii* contain promising molecules to inhibit the growth of cancer cells.

Further, the potential of *K. alvarezii* extract-encapsulated PEGylated liposomes were proven with mitochondrial transmembrane potential, ROS generation assay, acridine orange, ethidium bromide and DAPI staining methods. Triggering apoptosis in cancer cells can be proven by various methods where DAPI and acridine orange are considered as auspicious technique. Time-dependent increase of apoptosis with condensed nuclei was observed in HeLa and Caov-4 cell lines in association with DAPI staining (Prokhorova et al. 2018). Apoptotic effect of medicinal herb *Bacopa monnieri* was evaluated by Smith et al., with its purified extract (Smith et al. 2018). HT-29, SW480, SW620 and HCT116 cell lines were chosen to prove the role of medicinal extract on enhancing apoptotic body formation with acridine orange staining method (Kauntz et al. 2011).

Conclusions

Folate conjugated *K. alvarezii* extract-encapsulated PEGylated liposomes was formulated by thin-film hydration technique. PEGylated liposomes were significantly delivered the bioactive compounds of *K. alvarezii* extract into human adenoma MCF-7 breast cancer cells, inhibited the cell growth and induced apoptosis. The observed anticancer activity might be due to FR-receptor-targeted liposome internalization significantly increased the cellular uptake efficiency. In this study, folate conjugated liposomes were formulated by incorporating FA-PEG-DSPE/cholesterol/DSPC construct in the lipid bilayer and bioactive compounds of *K. alvarezii* was encapsulated. FA-conjugated *K. alvarezii* extract-encapsulated PEGylated liposomes have been found to possess controlled release characteristics with excellent physiological stability and biocompatibility. PEGylated liposomes were found to be 140 nm diameter, nearly spherical shape with + 0.2 mV zeta potential. Bioactive compounds of *K. alvarezii* extract released from PEGylated liposomes prompted the apoptosis by increasing ROS production, mitochondrial transmembrane potential damage/loss and morphological changes of the nucleus of MCF-7 cells. The outcomes of cellular up-take assay confirmed that FA-conjugated *K. alvarezii* extract-encapsulated PEGylated liposomes feasibly selected the target (folate receptor) cancer cells. Hence, further in vivo animal studies will be required to reveal the exact molecular mechanisms behind the apoptosis induced by FA-conjugated *K. alvarezii* extract-encapsulated PEGylated liposomes.

Compliance with ethical standards

Conflict of interest The authors declare no competing financial interest.

Ethical approval This article does not contain any studies with human participants performed by any of the authors. All applicable international, national, and/or institutional guidelines for the care and use of animals were followed.

Informed consent For this type of study, formal consent is not required.

References

Annamalai P, Thayman M, Rajan S, Raman LS, Ramasubbu S, Perumal P (2015) Ethyl acetate extract from marine sponge *Hyattella cribriformis* exhibit potent anticancer activity by promoting tubulin polymerization as evidenced mitotic arrest and induction of apoptosis. Pharmacogn Mag 11(42):345–355

Baskararaj S, Theivendren P, Palanisamy P, Kannan S, Pavadai P, Arunachalam S, Sankaranarayanan M, Mohan UP, Ramasamy L, Kunjiappan S (2019) Optimization of bioactive compounds extraction assisted by microwave parameters from *Kappaphycus alvarezii* using RSM and ANFIS modeling. J Food Meas Charact 13(4):2773–2789

Becker R, Frick A, Boderke P, Fürst C, Müller W, Tertsch K, Werner U, Loos P, Schöttle I (2011) Long-acting formulations of insulins. Google Patents

Bhalerao S, Raje Harshal A (2003) Preparation, optimization, characterization and stability studies of salicylicacid liposomes. Drug Dev Ind Pharm 29(4):451–467

Biswas S, Dodwadkar NS, Deshpande PP, Torchilin VP (2012) Liposomes loaded with paclitaxel and modified with novel triphenylphosphonium-PEG-PE conjugate possess low toxicity, target mitochondria and demonstrate enhanced antitumor effects in vitro and in vivo. J Control Release 159(3):393–402

Blume G, Cevc G (1990) Liposomes for the sustained drug release in vivo. Biochimica et Biophysica Acta (BBA)-Biomembranes 1029(1):91–97

Bray F, Ferlay J, Soerjomataram I, Siegel RL, Torre LA, Jemal A (2018) Global cancer statistics 2018: GLOBOCAN estimates of incidence and mortality worldwide for 36 cancers in 185 countries. CA 68(6):394–424

Chang V-S, Okechukwu PN, Teo S-S (2017) The properties of red seaweed (*Kappaphycus alvarezii*) and its effect on mammary carcinogenesis. Biomed Pharmacother 87:296–301

Cho H-Y, Lee CK, Lee Y-B (2015) Preparation and evaluation of PEGylated and folate-PEGylated liposomes containing paclitaxel for lymphatic delivery. J Nanomater 16(36):1–10

Chowdhury A, Kunjiappan S, Panneerselvam T, Somasundaram B, Bhattacharjee C (2017) Nanotechnology and nanocarrier-based

approaches on treatment of degenerative diseases. Int Nano Lett 7(2):91–122

Dash V, Mishra SK, Singh M, Goyal AK, Rath G (2010) Release kinetic studies of aspirin microcapsules from ethyl cellulose, cellulose acetate phthalate and their mixtures by emulsion solvent evaporation method. Sci Pharm 78(1):93–102

Đorđević V, Balanč B, Belščak-Cvitanović A, Lević S, Trifković K, Kalušević A, Kostić I, Komes D, Bugarski B, Nedović V (2015) Trends in encapsulation technologies for delivery of food bioactive compounds. Food Eng Rev 7(4):452–490

Elzainy AA, Gu X, Simons FER, Simons KJ (2005) Hydroxyzine and cetirizine-loaded liposomes: effect of duration of thin film hydration, freeze-thawing and changing buffer pH on encapsulation and stability. Drug Dev Ind Pharm 31(3):281–291

Ferraces-Casais P, Lage-Yusty M, De Quirós AR-B, López-Hernández J (2012) Evaluation of bioactive compounds in fresh edible seaweeds. Food Anal Methods 5(4):828–834

Gabizon AA (2001) Pegylated liposomal doxorubicin: metamorphosis of an old drug into a new form of chemotherapy. Cancer Invest 19(4):424–436

Gabizon A, Horowitz AT, Goren D, Tzemach D, Mandelbaum-Shavit F, Qazen MM, Zalipsky S (1999) Targeting folate receptor with folate linked to extremities of poly (ethylene glycol)-grafted liposomes: *In vitro* studies. Bioconjug Chem 10(2):289–298

Ganesan V, Gurumani V, Kunjiappan S, Panneerselvam T, Somasundaram B, Kannan S, Chowdhury A, Saravanan G, Bhattacharjee C (2018) Optimization and analysis of microwave-assisted extraction of bioactive compounds from *Mimosa pudica L.* using RSM & ANFIS modeling. J Food Meas Charact 12(1):228–242

Ghannam A, Abbas A, Alek H, Al-Waari Z, Al-Ktaifani M (2013) Enhancement of local plant immunity against tobacco mosaic virus infection after treatment with sulphated-carrageenan from red alga (Hypnea musciformis). Physiol Mol Plant Pathol 84:19–27

Gijsens A, Derycke A, Missiaen L, De Vos D, Huwyler J, Eberle A, de Witte P (2002) Targeting of the photocytotoxic compound AlPcS4 to Hela cells by transferrin conjugated PEGlyated liposomes. Int J Cancer 101(1):78–85

Gutiérrez-Rodríguez AG, Juarez-Portilla C, Olivares-Banuelos T, Zepeda RC (2018) Anticancer activity of seaweeds. Drug Discov Today 23(2):434–447

Harris JM, Chess RB (2003) Effect of pegylation on pharmaceuticals. Nat Rev Drug Discovery 2(3):214–221

Hattori Y, Shimizu S, Ozaki K-i, Onishi H (2019) Effect of cationic lipid type in Folate-PEG-modified cationic liposomes on folate receptor-mediated siRNA transfection in tumor cells. Pharmaceutics 11(4):181–203

Hidalgo A, Ferraretto A, De Noni I, Bottani M, Cattaneo S, Galli S, Brandolini A (2018) Bioactive compounds and antioxidant properties of pseudocereals-enriched water biscuits and their in vitro digestates. Food Chem 240:799–807

Jain KK (2017) Nanooncology. In: The Handbook of Nanomedicine. Humana Press, Springer, Berlin, pp 321–420

Jiménez Escrig A, Jiménez Jiménez I, Pulido R, Saura Calixto F (2001) Antioxidant activity of fresh and processed edible seaweeds. J Sci Food Agric 81(5):530–534

Kauntz H, Bousserouel S, Gossé F, Raul F (2011) Silibinin triggers apoptotic signaling pathways and autophagic survival response in human colon adenocarcinoma cells and their derived metastatic cells. Apoptosis 16(10):1042–1053

Klibanov AL, Maruyama K, Torchilin VP, Huang L (1990) Amphipathic polyethyleneglycols effectively prolong the circulation time of liposomes. FEBS Lett 268(1):235–237

Kumar KS, Ganesan K, Rao PS (2008) Antioxidant potential of solvent extracts of *Kappaphycus alvarezii* (Doty) Doty–An edible seaweed. Food Chem 107(1):289–295

Kumar P, Tambe P, Paknikar KM, Gajbhiye V (2017) Folate/N-acetyl glucosamine conjugated mesoporous silica nanoparticles for targeting breast cancer cells: a comparative study. Colloids Surf B 156:203–212

Kunjiappan S, Bhattacharjee C, Chowdhury R (2015) In vitro antioxidant and hepatoprotective potential of *Azolla microphylla* phytochemically synthesized gold nanoparticles on acetaminophen–induced hepatocyte damage in *Cyprinus carpio L.*. In Vitro Cell Dev Biol Anim 51(6):630–643

Kunjiappan S, Panneerselvam T, Somasundaram B, Arunachalam S, Sankaranarayanan M, Parasuraman P (2018a) Preparation of liposomes encapsulated epirubicin-gold nanoparticles for tumor specific delivery and release. Biomed Phys Eng Exp 4(4):045027

Kunjiappan S, Panneerselvam T, Somasundaram B, Sankaranaranan M, Parasuraman P, Joshi SD, Arunachalam S, Murugan I (2018b) Design, graph theoretical analysis and *in silico* modeling of *Dunaliella bardawil* biomass encapsulated N-succinyl chitosan nanoparticles for enhanced anticancer activity. Anticancer Agents Med Chem 18(13):1900–1918

Kunjiappan S, Theivendren P, Sankaranarayanan M, Somasundaram B, Subbarayan S, Arunachalam S, Parasuraman P, Sivakumar V, Murugan I, Baskararaj S (2018c) Design, graph theoretical analysis and bioinformatic studies of Proanthocyanidins encapsulated ethylcellulose nanoparticles for effective anticancer activity. Biomed Phys Eng Exp 5:025004

Kunjiappan S, Panneerselvam T, Govindaraj S, Parasuraman P, Baskararaj S, Sankaranarayanan M, Arunachalam S, Babkiewicz E, Jeyakumar A, Lakshmanan M (2019a) Design, *in silico* modelling and functionality theory of novel folate receptor targeted rutin encapsulated folicacid conjugated keratin nanoparticles for effective cancer treatment. Anticancer Agents Med Chem 19(16):1966–1982

Kunjiappan S, Theivendran P, Baskararaj S, Sankaranarayanan B, Palanisamy P, Saravanan G, Arunachalam S, Sankaranarayanan M, Natarajan J, Somasundaram B (2019b) Modeling a pH-sensitive Zein-co-acrylicacid hybrid hydrogels loaded 5-fluorouracil and rutin for enhanced anticancer efficacy by oral delivery. 3 Biotech 9(5):185–205

Lappalainen K, Jääskeläinen I, Syrjänen K, Urtti A, Syrjänen S (1994) Comparison of cell proliferation and toxicity assays using two cationic liposomes. Pharm Res 11(8):1127–1131

Li W, Szoka FC (2007) Lipid-based nanoparticles for nucleic acid delivery. Pharm Res 24(3):438–449

Li Y, Chen R, Li Y, Sharafudeen K, Liu S, Wu D, Wu Y, Qin X, Qiu J (2015) Folic acid-conjugated chromium (III) doped nanoparticles consisting of mixed oxides of zinc, gallium and tin and possessing near-infrared and long persistent phosphorescence for targeted imaging of cancer cells. Microchim Acta 182(9–10):1827–1834

Liao C, Xu D, Liu X, Fang Y, Yi J, Li X, Guo B (2018) Iridium (III) complex-loaded liposomes as a drug delivery system for lung cancer through mitochondrial dysfunction. Int J Nanomed 13:4417–4431

Low PS, Antony A (2004) Folate receptor-targeted drugs for cancer and inflammatory diseases. Adv Drug Deliv Rev 56(8):1055–1058

Malam Y, Loizidou M, Seifalian AM (2009) Liposomes and nanoparticles: nanosized vehicles for drug delivery in cancer. Trends Pharmacol Sci 30:592–599

McClements DJ, Decker EA, Park Y, Weiss J (2009) Structural design principles for delivery of bioactive components in nutraceuticals and functional foods. Crit Rev Food Sci Nutr 49(6):577–606

Persidis A (1999) Cancer multidrug resistance. Nat Biotechnol 17(1):94

Prokhorova EA, Kopeina GS, Lavrik IN, Zhivotovsky B (2018) Apoptosis regulation by sub-cellular relocation of caspases. Sci Rep 8(1):12199–12210

Prokop A, Davidson JM (2008) Nanovehicular intracellular delivery systems. J Pharm Sci 97(9):3518–3590

Pun SH, Tack F, Bellocq NC, Cheng J, Grubbs BH, Jensen GS, Davis ME, Brewster M, Janicot M, Janssens B (2004) Targeted delivery of RNA-cleaving DNA enzyme (DNAzyme) to tumor tissue by transferrin-modified, cyclodextrin-based particles. Cancer Biol Ther 3(7):641–650

Qiu L, Jing N, Jin Y (2008) Preparation and in vitro evaluation of liposomal chloroquine diphosphate loaded by a transmembrane pH-gradient method. Int J Pharm 361(1–2):56–63

Riganti C, Voena C, Kopecka J, Corsetto PA, Montorfano G, Enrico E, Costamagna C, Rizzo AM, Ghigo D, Bosia A (2011) Liposome-encapsulated doxorubicin reverses drug resistance by inhibiting P-glycoprotein in human cancer cells. Mol Pharm 8(3):683–700

Sato Y, Morimoto K, Hirayama M, Hori K (2011) High mannose-specific lectin (KAA-2) from the red alga *Kappaphycus alvarezii* potently inhibits influenza virus infection in a strain-independent manner. Biochem Biophys Res Commun 405(2):291–296

Shimizu Y (1985) Bioactive marine natural products with emphasis on handling of water-soluble compounds. J Nat Prod 48(2):223–235

Singh R, Lillard JW Jr (2009) Nanoparticle-based targeted drug delivery. Exp Mol Pathol 86(3):215–223

Sithranga Boopathy N, Kathiresan K (2010) Anticancer drugs from marine flora: an overview. J Oncol 2010:1–18

Smith E, Palethorpe H, Tomita Y, Pei J, Townsend A, Price T, Young J, Yool A, Hardingham J (2018) The purified extract from the medicinal plant *Bacopa monnieri*, bacopaside II, inhibits growth of colon cancer cells in vitro by inducing cell cycle arrest and apoptosis. Cells 7(7):81–92

Solis-Gonzalez OA (2014) Aggregation and elastic properties of poly (ethylene oxide)-block-poly (butylene oxide) polymersomes. PhD thesis, University of Sheffield

Suganya AM, Sanjivkumar M, Chandran MN, Palavesam A, Immanuel G (2016) Pharmacological importance of sulphated polysaccharide carrageenan from red seaweed *Kappaphycus alvarezii* in comparison with commercial carrageenan. Biomed Pharmacother 84:1300–1312

Sun C, Sze R, Zhang M (2006) Folicacid-PEG conjugated superparamagnetic nanoparticles for targeted cellular uptake and detection by MRI. J Biomed Mater Res Part A 78(3):550–557

Torchilin VP (2005) Recent advances with liposomes as pharmaceutical carriers. Nat Rev Drug Discov 4(2):145–160

Van Steenis J, Van Maarseveen E, Verbaan F, Verrijk R, Crommelin D, Storm G, Hennink W (2003) Preparation and characterization of folate-targeted PEG-coated PDMAEMA-based polyplexes. J Control Release 87(1–3):167–176

Wang H, Zhou L, Xie K, Wu J, Song P, Xie H, Zhou L, Liu J, Xu X, Shen Y (2018) Polylactide-tethered prodrugs in polymeric nanoparticles as reliable nanomedicines for the efficient eradication of patient-derived hepatocellular carcinoma. Theranostics 8(14):3949–3963

Xie J, Yang Z, Zhou C, Zhu J, Lee RJ, Teng L (2016) Nanotechnology for the delivery of phytochemicals in cancer therapy. Biotechnol Adv 34(4):343–353

Yaakob Z, Ali E, Zainal A, Mohamad M, Takriff MS (2014) An overview: Biomolecules from microalgae for animal feed and aquaculture. J Biol Res Thessalon 21(1):6–16

Yoo HS, Park TG (2004) Folate-receptor-targeted delivery of doxorubicin nano-aggregates stabilized by doxorubicin–PEG–folate conjugate. J Control Release 100(2):247–256

Yousefi A, Esmaeili F, Rahimian S, Atyabi F, Dinarvand R (2009) Preparation and *in vitro* evaluation of a pegylated nano-liposomal formulation containing docetaxel. Sci Pharm 77(2):453–464

Zhao X, Li H, Lee RJ (2008) Targeted drug delivery via folate receptors. Expert Opin Drug Deliv 5(3):309–319

Zhu Q, Feng C, Liao W, Zhang Y, Tang S (2013) Target delivery of MYCN siRNA by folate-nanoliposomes delivery system in a metastatic neuroblastoma model. Cancer Cell Int 13(1):65–71

Affiliations

Suraj Baskararaj[1] · **Theivendren Panneerselvam**[2] · **Saravanan Govindaraj**[3] · **Sankarganesh Arunachalam**[1] ·
Pavadai Parasuraman[4] · **Sureshbabu Ram Kumar Pandian**[1] · **Murugesan Sankaranarayanan**[5] · **Uma Priya Mohan**[1] ·
Ponnusamy Palanisamy[6] · **Vigneshwaran Ravishankar**[1] · **Selvaraj Kunjiappan**[1]

[1] Department of Biotechnology, Kalasalingam Academy of Research and Education, Krishnankoil, Virudhunagar, Tamilnadu 626126, India

[2] Department of Pharmaceutical Chemistry, Saraswathi College of Pharmacy, NH-24, Anwarpur, Pilkhuwa, Hapur, Uttar Pradesh 245304, India

[3] Department of Pharmaceutical Chemistry, MNR College of Pharmacy, Fasalwadi, Sangareddy, Telangana 502294, India

[4] Department of Pharmaceutical Chemistry, Faculty of Pharmacy, M.S. Ramaiah University of Applied Sciences, M S R Nagar, Bengaluru, Karnataka 560054, India

[5] Department of Pharmacy, Birla Institute of Technology and Science, Pilani, Rajasthan 333031, India

[6] School of Mechanical Engineering, Vellore Institute of Technology, Vellore, Tamilnadu 632014, India